SPRAY CHARACTERIZATION OF HIGH PRESSURE WATER MIST INJECTORS: EXPERIMENTAL AND THEORETICAL ANALYSIS

Paolo E. Santangelo[*,°,1], Ning Ren[*], Paolo Tartarini[°], André W. Marshall[*]

[*]Dept. of Fire Protection Engineering, University of Maryland, 3104 J.M. Patterson Bldg.,
College Park, MD 20742, USA
[°]Dept. of Mechanical and Civil Engineering, University of Modena and Reggio Emilia, Via Vignolese 905/b,
41100 Modena, Italy
[1]Corresponding author. E-mail: paoloemilio.santangelo@unimore.it, Tel.: +39 059 205 6101,
Fax: +39 059 205 6126

ABSTRACT

This study is focused on characterizing the spray released by a water mist injector at high pressure. To this end, an experimental campaign has been performed employing non intrusive techniques to investigate both drop size and initial velocity over a prescribed range of operative pressure. In particular, a laser-diffraction-based instrument (*Malvern Spraytec*) has been used to determine the characteristic diameter. An alternative method has been developed to reconstruct the drop-size trend in respect to fluid fraction: drop-size data have been averaged through mass flux distribution. This latter parameter has been measured by a mechanical patternator *ad hoc* built. Moreover a classic predictive formula for Sauter Mean Diameter has been validated through a physical analysis based on inviscid-fluid assumption. Velocity field has been studied by PIV technique. The proposed measurement methodology has been discussed and both maps and values have been finally stressed out. An experimental evaluation of the spray cone angle has been realized as an additional result of the PIV tests.

INTRODUCTION

Water mist fire suppression systems have become a promising technology in the fire fighting field, especially since halons have been banned. They are now mainly employed for residential and industrial units, but even aeronautic and naval fields seem to be interested in them. As far as such systems are relatively new, strong efforts have been spent to perform research on them. Among all the works available in the open literature it is worth to mention the studies realized by the US Navy [1-3] to evaluate water mist performances for shipboard applications. Other fundamental analyses have been carried out by Lentati and Chelliah [4], Grant et al. [5] and Chelliah [6] in order to investigate physical phenomena occurring in fire suppression with water mist. Most of the works [1-4,6-8] are focused on suppression mechanism and fluid-flame interaction: several studies were aimed at analyzing suppression performances, but only limited researches [5] have been conducted to investigate sprays in these systems. Transport phenomena in water mist sprays are generally characterized by high pressure injection (> 35 bar) and relatively small drops (characteristic diameter D_{v50} lower than 100 μm). The real advantage of these two features is the capability of spreading water droplets over a large area, while difficulties arise in interacting with fire and in overtaking potential obstructions. Transport and suppression depend on atomization and dispersion characteristics of spray. This work is aimed to investigate drop size and initial velocity at high operative pressures (> 50 bar). High values of pressure seem to be particularly interesting for the market because of the high suppression effectiveness they provide. High pressure sprays have been largely investigated for several applications and different fluids. Among the others, Yule and Widger [9] have studied water sprays produced by swirl atomizers, Senecal et al. [10]

the linear stability of a high speed viscous liquid sheet and Sovani et al. [11] the effect of ambient pressure on spray cone angle.

A typical high pressure water mist nozzle (645 J12C B1 by *PNR Italia S.r.l.*) has been employed in order to perform the experimental campaign. This kind of nozzle is commonly used also in gas turbine field [12] in order to realize the cooling effect produced by water fog on turbine blades. Drop size is a parameter of interest to analyze sprays and many efforts have been spent in order to determine it both experimentally and theoretically. A fundamental work on this subject has been carried out by Azzopardi [13] to provide a basic understanding of the possible analyses. A strong input to these researches has been given by the engine industry focused on determining the size of fuel droplets injected in the combustion chamber. Among the several studies on this subject, it is worthwhile to mention the works performed by Lorenzetto and Lefebvre [14] about plain jet atomizers, by Yule et al. [15] about vaporizing sprays, by Babinsky and Sojka [16] about experimental, numerical and theoretical analysis of drop-size distribution and by Panchagnula and Sojka [17] about drop size and velocity of effervescent sprays. Drop-size measurements have been carried out using a laser-based device, the *Malvern Spraytec*. Laser diagnostics is now very common for many applications in fluid dynamics, as shown in [18], and especially in particle sizing [19]. The *Malvern Spraytec* has been employed by Chaker et al. [12] to measure drop size in gas turbine fogging and by Santangelo et al. [20] to perform a preliminary experimental analysis of water mist sprays, while Zhu and Chigier [21] have discussed a method to process data related to sprays. Optical techniques has been applied to spray characterization by Yule et al. [22], Corcoran et al. [23] and Gemci et al. [24]. Drop-size measurements have been coupled to mass-flux-distribution measurements in order to average the data given by the

Malvern Spraytec over this parameter and finally obtain the characteristic diameter. Mass-flux distribution has been determined using a mechanical patternator. Patternation measurements in sprays have already been mentioned by Sovani et al. [25] because of the necessity of having a quantitative feedback about dispersion.

Many atomization correlations have been developed to evaluate the characteristic size of droplets. These engineering correlations are summarized in [26], but they are mainly related to different applications (internal combustion engines, in particular) and to different fluids (gasoline, kerosene or fuels in general). Their validation for water mist systems is one of the aims of this study. To this end, a theoretical model has been developed following the one proposed in [26] about pressure swirl atomizers and, finally, a correlation has been validated showing promising results.

Initial velocity of the spray has been investigated and determined by Particle Image Velocimetry (PIV). This technique is now largely employed in fluid dynamics, but it has rarely been applied to the particular field of the present study. Widmann et al. [27] and Sheppard [28] have performed PIV tests on traditional sprinkler sprays, while Presser et al. [29] have studied the water mist flow over different kinds of obstacle. Many works have been carried out by PIV to analyze Gasoline Direct Injection (GDI) systems. Rottenkolber et al. [30] have focused on the interaction between spray droplets and ambient air; Driscoll et al. [31] have determined the velocity field for the two phases (air and fuel); Lee et al. [32,33] have coupled PIV experiments and entropy analysis to characterize the spray structure; Anderson et al. [34] have performed an experimental investigation by both PIV and *Malvern Spraytec* on applying electrostatic charge to fuel sprays. In the same field, Wu et al. [35] have studied the spray structure of alternative oxygenated fuels. Basic works have been performed by Bachalo [36] describing PIV as one of the experimental methods in multiphase flows, by Ikeda et al. [37] and Palero and Ikeda [38] applying uncertainty analysis and dropsize-based discrimination to study turbulence of a spray, by Sujith [39] employing PIV to study the interaction between sprays and acoustic fields and by Prosperi et al. [40] investigating the gas entrainment by a hollow cone spray at variable density conditions. Finally, it seems to be worthwhile to mention the works performed by Boëdec and Simoëns [41] on velocity fields of the two phases (droplets and gas) in high pressure sprays and by Pavlova et al. [42] on the behavior of a spray subjected to a synthetic jet actuator. In the present work a series of PIV tests have been run to determine the velocity field of the spray in the area right downstream the injector outlet. The primary purpose of this investigation was to determine the initial velocity of the spray and its gap in respect to the one obtained from the physical analysis. Moreover, an evaluation of the spray cone angle has been stressed out from the PIV maps.

1. EXPERIMENTAL FACILITY

An experimental facility has been built in order to carry out tests on the water mist spray. A high pressure nozzle (Fig. 1, no. 1) has been placed at 2 m height from the floor. This nozzle consists of 6 peripheral injectors and the central one. The formers have been blocked in order to focus the activity on a single injector: this procedure increases simplicity in running experiments without any lack of physical comprehension of phenomena. A tank (Fig. 1, no. 2), an electric pump (Fig. 1, no. 3) and a pressure gauge (Fig. 1, no. 4) have been installed to supply water at definite values of

pressure. Drop-size measurements have been conducted employing a *Malvern Spraytec* particle sizer (Fig. 1, no. 5). A data acquisition system has been provided (Fig. 1, no. 6). The frame of the *Spraytec* has been adjusted in order to have the laser beam at 1 m height from the floor. This means that drop-size measurements have been taken on an approximately circular plane, that lies perpendicular to the injector axis at 1 m distance from its exit.
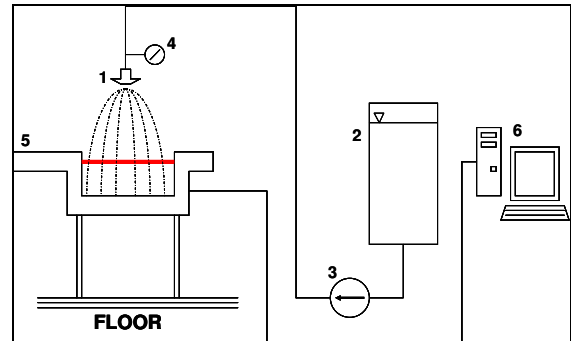

Fig. 1 – Sketch of the experimental facility.

Mass-flux measurements have been performed through a home made mechanical patternator, that has been built *ad hoc* (Fig. 2, no. 7). It is constituted by a set of 55 plastic tubes, each having an internal diameter of 18 mm and a thickness of 3 mm. The tubes are constrained in a straight row by two plastic beams; the plain of the entrance section of every tube has been made perpendicular to the injector axis. The frame of the patternator has been adjusted to collect water at 1 m height from the floor: this makes drop-size and mass-flux measurements consistent. The central tube has been placed right under the injector, so its axis was coincident with the injector one. This tube has been identified with number 0, so 27 tubes were placed along the negative direction of one diameter of the spray cross section and 27 along the positive one.

Velocity measurements have been conducted by Particle Image Velocimetry (PIV) technique. The laser emitter (Fig. 2, no. 8) and the camera (Fig. 2, no. 9) have been set in order to have the axis of the camera perpendicular to the emitted laser sheet.
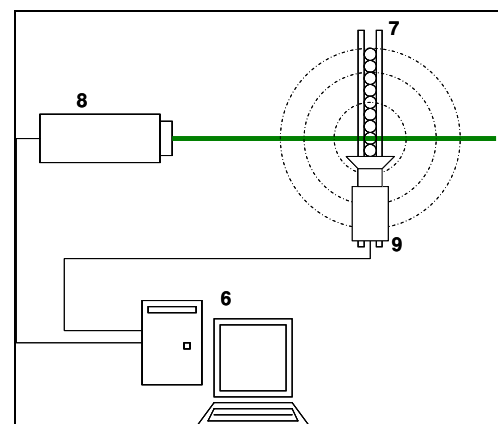

Fig. 2 – Sketch of patternator and PIV system
(view from above).

The PIV system (by *LaVision*) is constituted by a laser emitter (pulsed 30 mJ Nd:YAG), a thermo-electrically cooled CCD camera (14 bit, 4 Mpx) and a commercial software. The emitter has been set to fire the laser sheet along the plane

containing the injector axis. In particular, the frame has been adjusted to illuminate the initial region of the spray. Double images have been taken with a time distance of 5 µs between the two pictures of the same pair. Velocity maps have been reconstructed averaging a set of 300 double images taken at 4 Hz frequency.

The experimental campaign has been conducted over a range of high operative pressure. In particular, tests have been run at three values: 60, 70 and 80 bar. Working pressure is intended as the value reported by the pressure gauge, that means the pressure right upstream the nozzle.

2. EXPERIMENTAL METHODOLOGY

The sampling volume of the *Malvern Spraytec* would be enough wide to cover an entire diameter of the spray. Thus, placing the laser beam along a diameter may seem a sufficient way to carry out drop-size measurements, at a first glance. A possible problem that may occur is related to the difference between laser beam (a cylinder that may be identified as a line) and spray surface (a circle). *Malvern Spraytec* gives the curve Drop size vs. CVF (Cumulative Volume Fraction) as an output. As far as it is able to detect drop size only along a line, the ratio among different sizes over the entire surface of the spray might be missed. This effect may bias the curve above mentioned, if occurring. A simple procedure has been followed to check this inconvenience out. The *Malvern Spraytec* has been placed along a diameter and tests have been run varying length of the sampling volume. For each value of operative pressure, the SMD (Sauter Mean Diameter) decreased as length increased. SMD has been taken as a representative parameter: its variability proofs that measuring dropsize simply along a diameter yields biased results.

Therefore dropsize measurements have been taken at a prescribed number of locations along a radius (Fig. 3): this analysis is based on hypothesis of symmetry of the spray surface. Length of the sampling volume has been set equal to 30 mm and the *Malvern Spraytec* has been placed perpendicular to the testing radial coordinate. Location 0 is the one at the intersection between the radius and the injector axis, then measurements have been carried on every 30 mm along the radius. The last location has been set at 120 mm from location 0: further there is only mist, that is hardly caught by the *Malvern Spraytec*. It is worthwhile to mention that Zhu and Chigier [21] have proposed a mathematical method to convert linear dropsize measurements given by *Malvern Spraytec* to point measurements.

The second step to gain a proper experimental evaluation of drop size was to measure the mass flux distribution. To this end the mechanical patternator has been placed on a diameter and three tests for each value of working pressure have been run. Height of water in each tube yielded to mass flux, being the area of cross section and operative time *a priori* known. The obtained values have been considered to be valid for the entire circular crown identified by the generic tube (Fig. 3). This circular crown has a radial extension (Δr) that is equal to the outer diameter of each tube. So, it should be clearly stated that the radial distance between two consecutive location for drop-size measurement has been different from the radial length of any generic region related to mass-flux measurements. This fact has implied that a curve of mass-flux distribution has been finally extrapolated to obtain the values corresponding to the drop-size measurement locations.

Hypothesis of diametrical symmetry has been applied. Little asymmetries among tests referred to the same value of \pressure have brought in the opportunity of finding a center

of mass flux for each test. This point has been identified as the real center (real 0); its distance from the intersection between the injector axis and the spray surface is never greater than 18 mm.
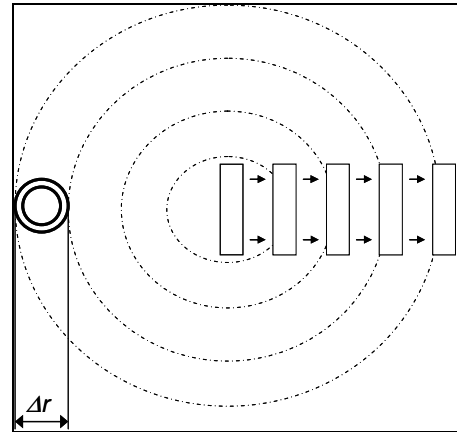

Fig. 3 – Sketch of the drop-size and mass-flux measurement procedure.

This procedure has allowed to build a series of curves for each value of operative pressure: positive and negative sides of the radial coordinate are defined in respect of the real center and they have been set the same way for every test. Figure 4 shows a set of 3 curves: each one is the result of averaging the mass flux distribution over all the tests at the same operative pressure. The spray appears to be very symmetric in respect to the real center and varying operative pressure seems to affect the peak (maximum value), but not the shape of the curve. This is consistent with the released-mass-flow increase as working pressure grows and tends to support the general statement that most of fluid flow (biggest droplets) is located in the spray cone, while tiny droplets (the proper mist) are spread in the surrounding space. These droplets can hardly be collected by the patternator because their motion is driven by the air streams and not by the imposed momentum.
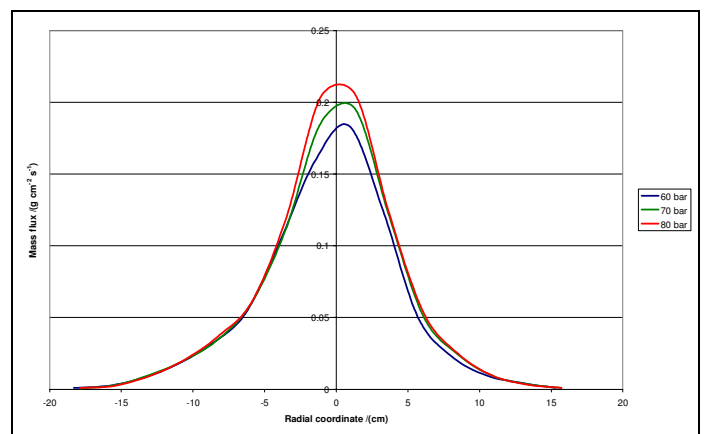

Fig. 3 – Average mass-flux distribution.

As already mentioned, the final step to reconstruct the Drop size vs. CVF curve has been to average drop-size measurements by mass flux distributions. This is a practical way to weigh drop-size data through a quantitative information; this procedure is aimed to correct the biasing effect previously described. To this end the mass-flux distribution curves have been mirrored in respect to *y* axis,

then they have been interpolated by a best approximation polynomial curve (3rd degree). One curve mass-flux distribution vs. radial positive coordinate has been gained for each value of working pressure through this procedure. These curves have been employed to average the drop-size point measurements by a simple integrating code.

The PIV experimental campaign has been conducted without addition of seeding to the investigated fluid. Water droplets released by a high pressure water mist injector are so tiny that they basically constitute tracking particles themselves. This statement is obviously acceptable once the liquid jet has been transformed into a spray jet (beyond the breakup location); moreover, the droplet concentration should be enough sparse to allow the software to reconstruct the pattern of each particle. These two conditions have implied that reliable values of velocity were practically obtained as of a distance of about 2 mm from the injector outlet along the axis. The laser sheet has been set to illuminate the plane containing the injector axis, so velocity measurements have taken into account velocity components lying on that plane.

The basic idea supporting a bi-dimensional measurement of a three-dimensional vectorial parameter is that tangential component tends to become negligible once the flow exits the injector. As far as the radius of the injector outlet is very tiny (1.5 mm), it is reasonable to state that angular velocity tends to decrease very fast once the generic particle (droplet) has been produced. This discussion leads to neglect the tangential component after a short axial distance from the injector outlet (around 5 mm). Therefore, velocity can be determined with good approximation by an experimental analysis on the already mentioned plane. Figure 4 shows a typical spray image during the PIV tests.
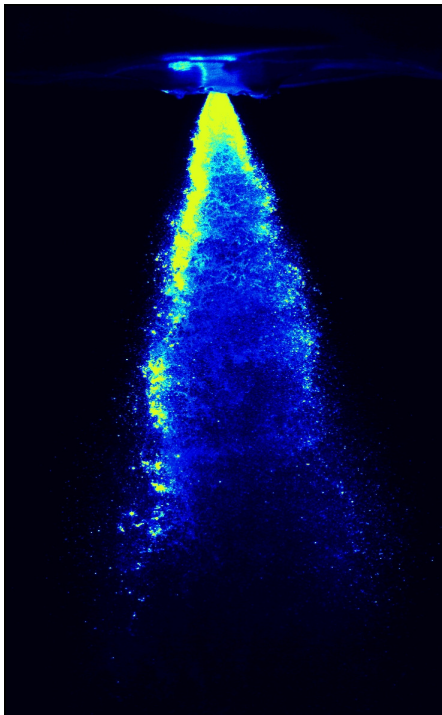

Fig. 4 – Spray image of PIV tests at 80 bar.

3. EXPERIMENTAL RESULTS

This averaging procedure has allowed to obtain a final set of reconstructed Drop size vs. CVF distributions. Finally the characteristic diameter has been determined from these data, being it defined either as D_{v50} or as SMD. It is worthwhile to

give an explicit expression of the Rosin-Rammler Log-normal distribution, which has been compared to the reconstructed Drop size vs. CVF curve:

$$CVF = \begin{cases} (2\pi 2^{-1/2} \int_0^{D_{CVF}} (\gamma' D)^{-1} e^{-\frac{[\ln(D/D_{v50})]^2}{2\gamma'^2}} dD & (D_{CVF} \leq D_{v50}), \\ 1 - e^{-0.693(D_{CVF}/D_{v50})^{\gamma}} & (D_{v50} < D_{CVF}), \end{cases}$$

(1)

where γ' is expressed as $\gamma' = 2((2\pi)^{1/2}(\ln 2)\gamma)^{-1}$. This formula has been employed to check the behavior of the predicted spray: it is shown that a curve-fitting coefficient $\gamma = 2.2 \div 2.3$ yields a good agreement between the Rosin-Rammler Log-normal distribution and the reconstructed curve. This expression has already been proposed by Wu et al. [43] for a study on traditional sprinkler sprays. The obtained data show a behavior that is consistent to the typical spray one: the values of γ are close to sprinkler ones and pressure appears not to affect the suitable value of γ.

Figure 5 shows a graphic example of these final experimental results, while figure 6 summarizes the trends of D_{v50} and SMD as functions of operative pressure.
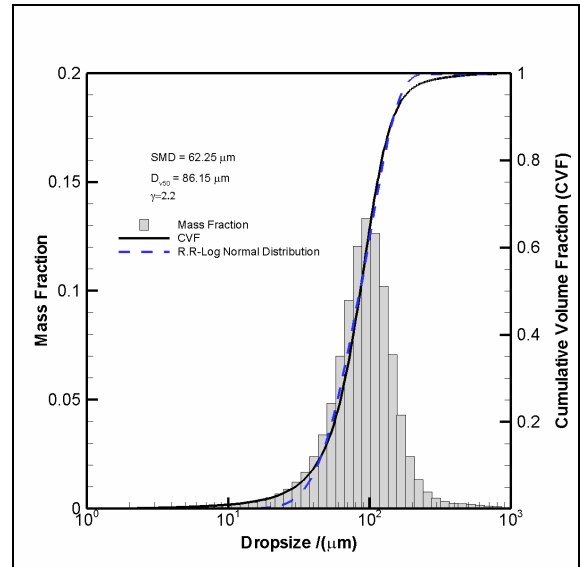

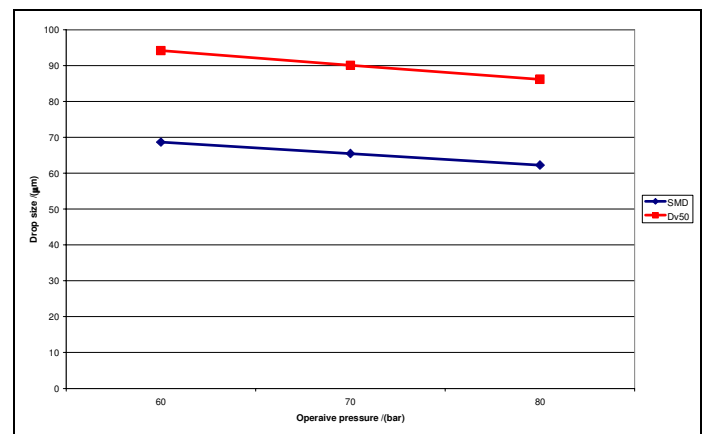Fig. 5 –Drop size vs. CVF distribution at 80 bar.

Fig. 6 – Characteristic diameter (SMD and D_{v50}) vs. Operative pressure.

The characteristic drop size tends to decrease as operative pressure increases: water mist systems emphasize their peculiarity as pumping pressure grows.

The most important result of the PIV experimental campaign is a set of velocity data for each value of operative pressure. Figure 7 shows an example of vector map with velocity magnitude. It is common over the investigated pressure range to have a strong flow in the conical region of the spray, which is characterized by highest velocity values. This flow is basically driven by the imposed momentum, while the proper mist is constituted by a number of tiny droplets in the peripheral sides of the cone: these are driven by air streams and they practically float at lower velocity. This fact was pointed out also in section 2 in respect of mass-flux distribution (Fig. 3).
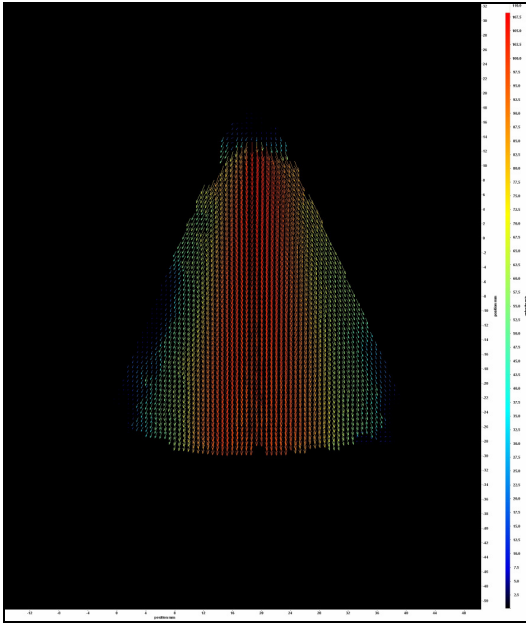

Fig. 7 – Velocity field with magnitude at 80 bar.

Figure 8 shows initial velocity magnitude compared to reference velocity at the outlet of the injector, which has been calculated through an inviscid model (see section 4).
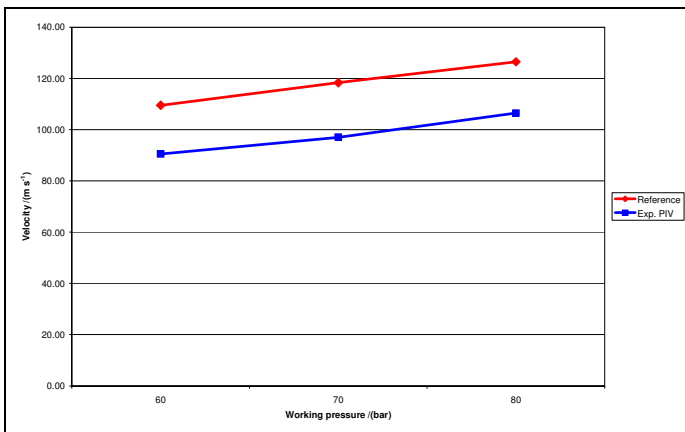

Fig. 8 – Experimental vs. Reference velocity magnitude.

The experimental PIV values correspond to a distance of 5 mm from the injector outlet: velocity cannot be easily reconstructed more closer to the exit because droplet concentration is too high to allow the software to clearly follow each pattern. Moreover, the breakup occurs in the first

2 mm and the hypothesis of negligible tangential component stated in section 3 becomes more weak the more close particles are to the outlet. The central zone (around 5 mm) at 10 mm is characterized by highest velocity, which is slightly above 80% of reference velocity. This peak does not show a strong decay while moving along the injector axis: velocity lightly decreases, but the flow is spread over a longer length. This latter statement is consistent to the conical geometry of the spray and seems to support the statement of conservation of momentum, without significant friction losses due to interaction with surrounding air.

An evaluation of the spray cone angle has been performed through the PIV vector maps. Figure 9 shows the evolution of this parameter along the axial coordinate. Location 0 corresponds to the initial share of the investigated area (from 0.39 to 10 mm from the outlet), location 1 corresponds to the central region (from 10 to 30 mm) and location 2 corresponds to the further share (from 30 to 40 mm).
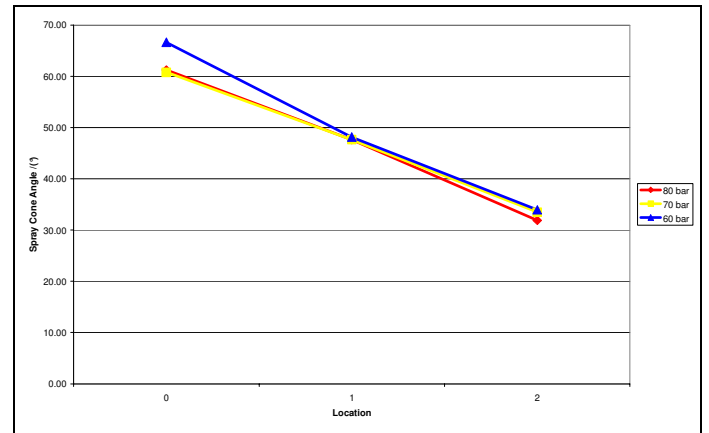

Fig. 9 – Spray cone angle over various locations along the injector axis.

Operating pressure in the prescribed range does not have a strong effect on the cone angle: initial values are greater than 60°, then they decrease to slightly less than 50° and they finally drop down to almost 30°. This behavior is consistent to the classical sprays produced by pressure swirl atomizers [26]: cone angle tends to decrease along the axial coordinate because of the interaction between sprayed and surrounding fluid, which becomes more strong the further droplets are from the outlet.

4. PHYSICAL ANALYSIS

A theoretical approach has been performed to validate a predictive formula for the characteristic diameter of the spray by the already described experimental data. A schematic geometry of the injector (Fig. 10) has been adopted to apply a physical approach.

Water flows with back straight motion between sections 0 and 1: this the injector slot and it is sloped at an angle ϕ in respect to the axis. The path between sections 1 and 2 (exit) is the swirl chamber: it is basically a convergent-divergent duct, that has a final inclination of θ in respect to the axis. Following the discussion proposed by Lefebvre [26] about pressure swirl atomizers, a Bernoulli equation has been introduced:

$$P = p_1 - p_{atm} + \frac{1}{2}\rho_L V_1^2 = p_2 - p_{atm} + \frac{1}{2}\rho_L V_2^2. \qquad (2)$$
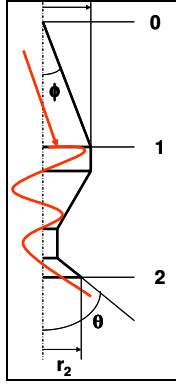
Fig. 10 – Sketch of the internal geometry of the injector (red line roughly represents the fluid trajectory).

As far as the assumption of inviscid fluid has been implicitly stated, total pressure is constant along the path 0-2. This pressure could have been measured by a Pitot tube at any location of the path, but the experimental facility has been conveniently endowed by a pressure gauge at section 0. This device measures static pressure in respect of the atmospheric one. Therefore, another simplifying hypothesis has been added: as far as dynamic load at section 0 is considered to be negligible, the value measured by the pressure gauge is assumed to be representative of total pressure.

Thus an expression for velocity at the outlet is yielded by equation 2:

$$V_2 = \left(\frac{2p_{PG}}{\rho_L} \right)^{1/2}. \tag{3}$$

The definition of the discharge coefficient has been borrowed from the internal combustion engine field. This coefficient can be used for any kind of nozzle or injector and represents the ratio between the effective area of fluid transit and the geometric cross section of the orifice:

$$C_D = \frac{A_F}{A_{TOT}}, \qquad C_D \in [0,1]. \tag{4}$$

At this point an expression for mass flow rate has been easily obtained from equations (3) and (4):

$$\dot{m}_L = \rho_L A_F V_2 = \rho_L C_D A_{TOT} V_2 = C_D A_{TOT} (2\rho_L p_{PG})^{1/2}. \tag{5}$$

The crucial point has become to determine the discharge coefficient, because the other parameters have been either *a priori* known (area of the outlet), or measured (pressure), or detected from technical tables (density). To this end an additional parameter should be introduced: the flow number, commonly used in the water mist field. It is defined as follows:

$$FN = \frac{Q}{p_{PG}^{1/2}} \tag{6}$$

and it has been measured by collecting the amount of water flown over a prescribed time at a known value of operative pressure. Flow number is reasonably constant as pressure varies. The relation between flow number and discharge coefficient is the key to gain this latter and finally the mass flow rate:

$$A_F = FN \left(\frac{\rho_L}{2} \right)^{1/2}, \tag{7}$$

$$C_D = \frac{FN}{A_{TOT}} \left(\frac{\rho_L}{2} \right)^{1/2}. \tag{8}$$

Mass flow rate has been calculated as a result of the described procedure. Table 1 summarizes the values of involved parameters showing schematically the steps of this discussion.

Table 1: Parameters of the physical approach.

Operative pressure [Pa] $\times 10^{-5}$	60	70	80
FN [m$^{7/2}$ kg$^{-1/2}$] $\times 10^8$	1.00	1.00	1.00
$C_D \times 10^2$	3.35	3.35	3.35
$A_{TOT} \times 10^6$ [m^2]	7.07	7.07	7.07
Density [kg m^{-3}]	999.97	999.97	999.97
Mass flow rate $\times 10^2$ [kg s^{-1}]	2.45	2.65	2.83

As a last step, a correlation has been validated to predict the characteristic drop size of the spray. Many correlation are available in the scientific literature about high pressure sprays. They mostly involve the SMD as the characteristic diameter. They have been developed for fuels (gasoline, kerosene, etc.) rather than other fluids, because they are results of studies in the combustion engine or gas turbines field. In particular, the classic correlation proposed by Radcliffe [26,44] has shown promising agreement for water mist sprays:

$$SMD = 7.3 \cdot \sigma^{0.6} \cdot \nu^{0.2} \cdot \dot{m}_L^{0.25} \cdot p_L^{-0.4}. \tag{9}$$

It is clearly a crude correlation, because it reports dimensional parameters, which are strongly connected to the nature of the fluid. Figure 10 shows the trend of experimental and predicted SMD as a function of operative pressure.
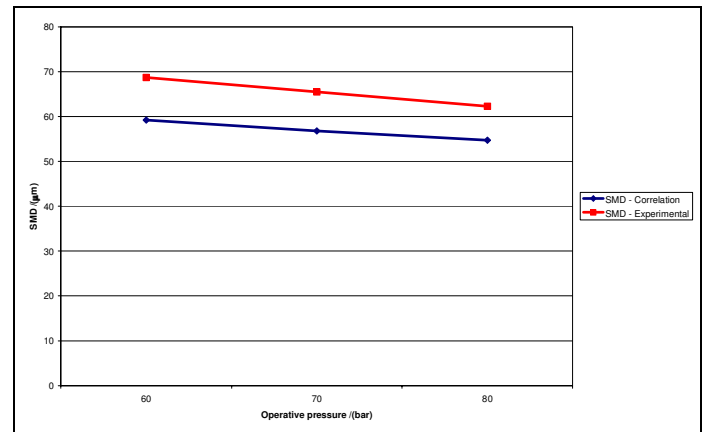

Fig. 10 – SMD vs. Operative pressure: comparison between experimental and predicted data.

The validated correlation tends to underestimate the SMD with a relative error lower than 15%. Moreover, the trends of experimental and predicted SMD are very consistent one to the other.

CONCLUSIONS

The present work has been focused on characterizing a high pressure spray produced by a water mist injector. The engineering application field is mainly fire suppression, where water mist systems seem to represent one of the most promising technologies, but the results could be extended to the broad area of high pressure sprays (cooling techniques, fuel injection, etc.). Many ideas inspiring this research are shared with gas turbine and internal combustion engine fields.

Optical techniques have been employed to conduct the experimental campaign. A light-diffraction-based instrument (*Malvern Spraytec*) has been used to determine the characteristic drop size of the spray. However, this kind of measurement has been performed through an innovative methodology based on averaging particle sizing data over mass flux distribution. This latter parameter has been measured by an *ad hoc* built mechanical patternator. Experimental Drop size vs. CVF distribution has been stressed out for each imposed working pressure; a suitable value for parameter γ has been proposed to match a Rosin-Rammler Log-normal distribution with the experimental one. A physical analysis based on inviscid-fluid assumption has been proposed to validate a classical predictive correlation for a characteristic diameter (SMD): this correlation has shown good agreement with experimental results.

Velocity measurements of the initial spray have been performed through PIV technique. The procedure has been analyzed through a geometrical and physical discussion. Velocity magnitude trend has shown that this parameter does not decrease significantly along the injector axis: this means that friction losses with surrounding air are not effective at high operative pressure. Non-dimensional velocity is almost constant in respect to working pressure: initial magnitude is almost 80% of reference velocity, that is related to the inviscid model. Velocity distribution has shown that the central region of the spray cone is practically driven by imposed momentum, while the proper mist (tiny droplets) lies in the peripheral zone and is driven by buoyancy.

Moreover, an evaluation of spray cone angle has been derived from PIV vector maps. This parameter does not have strong variation in respect of operative pressure and its trend along the injector axis is consistent with typical pressure swirl atomizers: it tends to decrease because of sprayed fluid interaction with surrounding air.

ACKNOWLEDGMENTS

NOMENCLATURE

Symbol	Quantity	SI Unit
A	Area	m^2
C_D	Discharge coefficient	
CVF	Cumulative Volume Fraction	
D	Drop size	μm
D_{v50}	Characteristic diameter	μm
FN	flow number	$m^{7/2} kg^{-1/2}$
$\dot{m}$	mass flow rate	$kg\ s^{-1}$
P	static pressure	Pa
P	total pressure	Pa
Q	volumetric flow rate	$m^3\ s^{-1}$
SMD	Sauter Mean Diameter	μm
V	velocity magnitude	$m\ s^{-1}$

Greek symb.

γ	curve fitting coefficient	
$\dot{\gamma}$	Parameter in Eq. (1)	
ν	kinematic viscosity	$m^2\ s^{-1}$
ρ	density	$kg\ m^{-3}$
σ	surface tension	$N\ m^{-1}$

Subscripts

0, 1, 2	sections of the injector
atm	atmospheric
CVF	Cumulative Volume Fraction
F	flow
L	liquid
PG	pressure gauge
TOT	total

REFERENCES

[1] C.C. Ndubizu, R. Ananth, P.A. Tatem and V. Motevalli, On water mist fire suppression mechanisms in a gaseous diffusion flame, *Fire Saf. J.*, vol. 31, pp. 253-276, 1998.

[2] K.C. Adiga, R.F. Hatcher Jr., R.S. Sheinson, F.W. Williams and S. Ayers, A computational and experimental study of ultra fine water mist as a total flooding agent, *Fire Saf. J.*, vol. 42, pp. 150-160, 2007.

[3] B.T. Fisher, A.R. Awtry, R.S. Sheinson and J.W. Fleming, Flow behavior impact on the suppression effectiveness of sub-10-μm water drops in propane/air co-flow non-premixed flames, *Proc. Combust. Inst.*, vol. 31, pp. 2731-2739, 2007.

[4] A.M. Lentati and H.K. Chelliah, Dynamics of water droplets in a counterflow field and their effect on flame extinction, *Combust. Flame*, vol. 115, pp. 158-179, 1998.

[5] G. Grant, J. Brenton and D. Drysdale, Fire suppression by water sprays, *Prog. Energ. Combust. Sci.*, vol. 26, pp. 79-130, 2000.

[6] H.K. Chelliah, Flame inhibition/suppression by water mist: droplet size/surface area, flame structure, and flow residence time effects, *Proc. Combust. Inst.*, vol. 31, pp. 2711-2719, 2007.

[7] G.O. Thomas, The quenching of laminar methane-air flames by water mists, *Combust. Flame*, vol. 130, pp. 147-160, 2002.

[8] T. Parra, F. Castro, C. Méndez, J.M. Villafruela and M.A. Rodríguez, Extinction of premixed methane-air flames by water mist, *Fire Saf. J.*, vol. 39, pp. 581-600, 2004.

[9] A.J. Yule and I.R. Widger, Swirl atomizers operating at high water pressure, *Int. J. Mech. Sci.*, vol. 38, pp. 981-999, 1996.

[10] P.K. Senecal, D.P. Schmidt, I. Nouar, C.J. Rutland, R.D. Reitz and M.L. Corradini, Modeling high-speed viscous liquid sheet atomization, *Int. J. Multiph. Flow*, vol. 25, pp. 1073-1097, 1999.

[11] S.D. Sovani, E. Chou, P.E. Sojka, J.P. Gore, W.A. Eckerle and J.D. Crofts, High pressure effervescent atomization: effect of ambient pressure on spray cone angle, *Fuel*, vol. 80, pp. 427-435, 2001.

[12] M. Chaker, C.B. Meher-Homji and T. Mee III, Inlet fogging of gas turbine engines – Part II: Fog droplet sizing analysis, nozzle types, measurements, and testing, *J. Eng. Gas Turbines Power – Trans. ASME*, vol. 126, pp. 559-570, 2004.

[13] B.J. Azzopardi, Measurement of drop sizes, *Int. J. Heat Mass Transf.*, vol. 22, pp. 1245-1279, 1979.

[14] G.E. Lorenzetto and A.H. Lefebvre, Measurements of drop size on a plain jet airblast atomizer, *AIAA J.*, vol. 15, pp. 1006-1010, 1977.

[15] A.J. Yule, P.R. Ereaut and A. Ungut, Droplet sizes and velocities in vaporizing sprays, *Combust. Flame*, vol. 54, pp. 15-22, 1983.

[16] E. Babinsky and P.E. Sojka, Modeling drop size distributions, *Prog. Energy Combust. Sci.*, vol. 28, pp. 303-329, 2002.

[17] M.V. Panchagnula and P.E. Sojka, Spatial droplet velocity and size profiles in effervescent atomizer-produced sprays, *Fuel*, vol. 78, pp. 729-741, 1999.

[18] B.S. Rinkevichius, Laser diagnostics in fluid mechanics, Begell House, New York City, NY, USA, 1998.

[19] N.E. Tayali and C.J. Bates, Particle sizing techniques in multiphase flows: A review, *Flow Meas. Instrum.*, vol. 1, pp. 77-105, 1990.

[20] P.E. Santangelo, N. Ren, P. Tartarini and A.W. Marshall, Discharge and dispersion analysis of water mist sprays, *Proc. XXV UIT National Heat Transfer Conference*, pp. 123-127, 2007.

[21] H.M. Zhu and N. Chigier, Tomographical transformation of Malvern measurements, *Int. Commun. Heat Mass Transf.*, vol. 13, pp. 483-491, 1986.

[22] A.J. Yule, C. Ah Seng, P.G. Felton, A. Ungut and N.A. Chigier, A laser tomographic investigation of liquid fuel sprays, *Symposium (International) on Combustion*, vol. 18, pp. 1501-1510, 1981.

[23] T.E. Corcoran, R. Hitron, W. Humphrey and N. Chigier, Optical measurement of nebulizer sprays: a quantitative comparison of diffraction, Phase Doppler interferometry, and time of flight techniques, *J. Aerosol Sci.*, vol. 31, pp. 35-50, 2000.

[24] T. Gemci, K. Yakut, N. Chigier and T.C. Ho, Experimental study of flash atomization of binary hydrocarbon liquids, *Int. J. Multiph. Flow*, vol. 30, pp. 395-417, 2004.

[25] S.D. Sovani, P.E. Sojka and A.H. Lefebvre, Effervescent atomization, *Prog. Energy Combust. Sci.*, vol. 27, pp. 483-521, 2001.

[26] A.H. Lefebvre, Atomization and Sprays, Hemisphere, New York City, NY, USA, 1989.

[27] J.F. Widmann, D.T. Sheppard and R.M. Lueptow, Non-Intrusive Measurements in Fire Sprinkler Sprays, *Fire Technol.*, vol. 37, pp. 297-315, 2001.

[28] D.T. Sheppard, Spray Characteristics of Fire Sprinklers, Ph.D. thesis, Northwestern University, Evanston, IL, USA, 2002.

[29] C. Presser, G. Papadopoulos and J.F. Widmann, PIV measurements of water mist transport in a homogeneous turbulent flow past an obstacle, *Fire Saf. J.*, vol. 41, pp. 580-604, 2006.

[30] G. Rottenkolber, J. Gindele, J., Raposo, K. Dullenkopf, W. Hentschel, S. Wittig, U. Spicher and W. Merzkirch, Spray analysis of a gasoline direct injector by means of two-phase PIV, *Exp. Fluids*, vol. 32, pp. 710-721, 2002.

[31] K.D. Driscoll, V. Sick and C. Gray, Simultaneous air/fuel-phase PIV measurements in a dense fuel spray, *Exp. Fluids*, vol. 35, pp. 112-115, 2003.

[32] K. Lee, C. Lee and Y. Joo, Application technique of particle image velocimetry and entropy analysis to investigate spray structure for gasoline direct injection injector, *Meas. Sci. Technol.*, vol. 14, pp. 953-964, 2003.

[33] K.H. Lee, C.H. Lee and C.S. Lee, An experimental study on the spray behavior and fuel distribution of GDI injectors using the entropy analysis and PIV method, *Fuel*, vol. 83, pp. 971-980, 2004.

[34] E.K. Anderson, A.P. Carlucci, A. De Risi and D.C. Kyritsis, Synopsis of experimentally determined effects of electrostatic charge on gasoline sprays, *Energy Conv. Manag.*, vol. 48, pp. 2762-2768, 2007.

[35] Z. Wu, Z. Zhu and Z. Huang, An experimental study on the spray structure of oxygenated fuel using laser-based visualization and particle image velocimetry, *Fuel*, vol. 85, pp. 1458-1464, 2006.

[36] W.D. Bachalo, Experimental methods in multiphase flows, *Int. J. Multiph. Flow*, vol. 20, pp. 261-295, 1994.

[37] Y. Ikeda, N. Yamada and T. Nakajima, Multi-intensity-layer particle-image velocimetry for spray measurement, *Meas. Sci. Technol.*, vol. 11, pp. 617-626, 2000.

[38] V.R. Palero and Y. Ikeda, Droplet-size-classified stereoscopic PIV for spray characterization, *Meas. Sci. Technol.*, vol. 13, pp. 1050-1057, 2002.

[39] R.I. Sujith, An experimental investigation of interaction of sprays with acoustic fields, *Exp. Fluids*, vol. 38, pp. 576-587, 2005.

[40] B. Prosperi, G. Delay, R. Bazile, J. Helie and H.J. Nuglish, FPIV study of gas entrainment by a hollow cone spray submitted to variable density, *Exp. Fluids*, vol. 43, pp. 315-327, 2007.

[41] T. Boëdec and S. Simoëns, Instantaneous and simultaneous planar velocity fields measurements of two phases for turbulent mixing of high pressure sprays, *Exp. Fluids*, vol. 31, pp. 506-518, 2001.

[42] A.A. Pavlova, K. Otani and M. Amitay, Active control of sprays using a single synthetic jet actuator, *Int. J. Heat Fluid Flow*, vol. 29, pp. 131-148, 2008.

[43] D. Wu, D. Guillemin and A.W. Marshall, A modeling basis for predicting the initial sprinkler spray, *Fire Saf. J.*, vol. 42, pp. 283-294, 2007.

[44] A. Radcliffe, Fuel Injection, High Speed Aerodynamics and Jet Propulsion, Princeton University Press, Princeton, NJ, USA, 1960.